Int J Clin Exp Med 2021;14(2):831-839
www.ijcem.com /ISSN:1940-5901/IJCEM0122318

Original Article

Imaging and pathologic characteristics of solid pseudopapillary tumor of pancreas

Jun Cui*, Li Tang*, Liu-Ye Huang

*Department of Gastroenterology, The Affiliated Yantai Yuhuangding Hospital of Qingdao University, Yantai 264000, Shandong, China. *Equal contributors.*

Received September 13, 2020; Accepted November 10, 2020; Epub February 15, 2021; Published February 28, 2021

Abstract: Objective: The imaging characteristics of solid pseudopapillary tumor of pancreas (SPTP) by color ultrasound, CT, MRI and endoscopic ultrasonography (EUS) were analyzed and compared with pathological results to explore methods of early diagnosis of SPTP. Methods: The color ultrasound, CT, MRI and EUS of SPTP of 30 SPTP cases confirmed by surgery and pathology were retrospectively analyzed to determine the location, size, shape, density, signal, and enhancement pattern of the tumor. The patients underwent EUS puncture biopsy before the operation. The specimen after surgical resection were examined by pathology and compared with the pathology. Results: The SPTP ultrasound of patients showed hypoechoic solid masses. CT findings mainly manifested as mixed density of cystic and solid shadows, with some solid structures showed papillary or wall nodular protrusions, and strengthened after enhancement. MRI showed heterogeneous mixed signals on T1WI and T2WI. The specific signs such as necrotic cystic degeneration and hemorrhage inside the tumor can be identified, and the solid parts of the tumor were enhanced progressively. The patients' EUS examination mainly showed hypoechoic solid masses with uneven internal echo. The pathological diagnosis was confirmed by EUS biopsy before surgery, which was consistent with the postoperative pathological results. Conclusion: Solid pseudopapillary tumor of the pancreas has certain imaging characteristics, with its pathological diagnosis can be confirmed by EUS biopsy postoperatively.

Keywords: Solid pseudopapillary tumor of pancreas, computed tomography, X-ray, magnetic resonance imaging (MRI)

Introduction

Solid pseudopapillary tumor of pancreas (SPTP) is a rare benign or low-grade pancreatic tumor which usually occurs in young women and may have the possibility of deterioration [1, 2]. Since SPTP has good prognosis after local surgical excision, its preoperative diagnosis is of great value in choosing surgical methods and evaluating the prognosis of patients [3]. Although the incidence rate of SPTP accounts for only 0.17%~3% of primary pancreatic tumors, its misdiagnosis rate can reach as high as 90%. Therefore, it is of great significance to summarize the preoperative imaging features of SPTP for guiding the clinical diagnosis [4]. The preoperative diagnosis of SPTP has contributed to the determination of surgical plan and the improvement of prognosis. At present, the diagnosis of SPTP is mainly based on the results of histopathology and immunohistochemistry. However, there is still a lack of clinical observation and research on relationship between preoperative imaging and clinicopathological features. This study retrospectively analyzed the imaging findings of 30 SPTP cases confirmed by surgery and pathology, and analyzed the characteristics of color ultrasound, CT, MRI and EUS and pathological basis, aiming to improve the diagnosis of the disease.

Data and methods

Clinical data

A total of 30 SPTP cases confirmed by surgery and pathology in our hospital between January 2004 and December 2018 were retrospectively analyzed. The study was approved by the Ethics Committee of our hospital.

Inclusive criteria and exclusive criteria

Inclusive criteria: The SPTP patients were confirmed by surgery and pathology. Patients with complete imaging examination data preoperatively. Patients completed at least one imaging examination. Patients voluntarily signed informed consent.

Exclusive criteria: Patients with incomplete clinical data; patients with other pancreatic tumor confirmed by postoperative pathology.

Research methods

The clinical data of the patients, including gender, age, preoperative imaging data, surgical methods, postoperative pathological examination results and follow-up, were collected by reading the cases and reviewing the relevant examination results, and the features of preoperative imaging diagnosis were summarized.

Examination methods

Abdominal ultrasonography: GE LOGIQ E9 color Doppler with 2-5 MHz broadband probe was adopted; the abdominal condition was settled, and the color gain was adjusted right before the noise appears. The size, shape, capsule, internal echo and blood flow distribution of pancreas were observed by 2D ultrasound to record the symptoms such as location, size, shape, boundary and internal echo of pancreatic mass.

Enhanced CT examination: All patients underwent CT scan and enhanced CT scan by lightspeed VCT 64-layer spiral CT scanner. The scanning ranged from the top of the diaphragm to below the uncinate process of pancreas. *Scanning Parameters:* 120 kV; 250-280 mA; both layer thickness and layer spacing were 5 mm; The contrast agent for enhanced scanning was Omnipaque; The contrast rate was 3.0-4.0 ml/s and 1.5 ml/kg, the arterial phase was 25 s, the portal vein phase was 60-70 s, and the phase delay was 120-160 s.

Enhanced MRI examination: GE Signa Excite 3.0 T was adopted for MRI scans. SPGR sequence, conventional T1WI, T2WI and DWI, T1WI and T2WI were added with SPIR. The thickness and spacing of layers were 5 mm and 2 mm respectively, and the matrix was 400×400; the dynamic enhanced scanning was performed by sequence of LAVA with thickness and spacing of layers at 3 mm and 1.5 mm respectively. The contrast agent for enhanced MRI scan was Magnevist (Gadopentate Meglumine Injection), with the dose of 0.1 ml/kg and rate of 2 ml/s. The first scan was performed 15 s after the injection via cubital vein. The scan was repeated 3 to 4 times, and the delayed scan was carried out 180 s later. The CT values of tumor regions of interest (0.5×0.5 cm) in plain scan, arterial phase and parenchymal phase were measured with vernier caliper. The area of liquefaction, cystoid variation, necrosis and calcification should be avoided for selection of ROI.

EUS-guided needle biopsy

Twelve patients underwent needle biopsy guided by Olympus GF-UCT240-type EUS. The puncture needle used was Echo Tip Ultra 19 G produced by COOK Corporation. The puncture specimens were subsequently examined by smear cytology and section histology.

Surgical approaches

The surgical methods should be determined on a basis of the location of the tumor and its invasion range. The surgical approaches included single tumor resection, distal pancreatectomy with/without splenectomy, and pancreaticoduodenectomy.

Pathological examination

The histopathological examination and immunohistochemical staining of vimentin, CK, NSE, CK8/18, CD10, CGA and syn were performed on the surgically removed specimens.

The observation of indexes

The imaging and pathological features of the patients were recorded. The comparative analysis were conducted between the CT values of arterial, parenchymal tumor tissues and normal pancreatic tissues, as well as the difference of CT values in patients with different CD10 expression.

Statistical analysis

The data results of the study were recorded into the statistical software SPSS 22.0. The

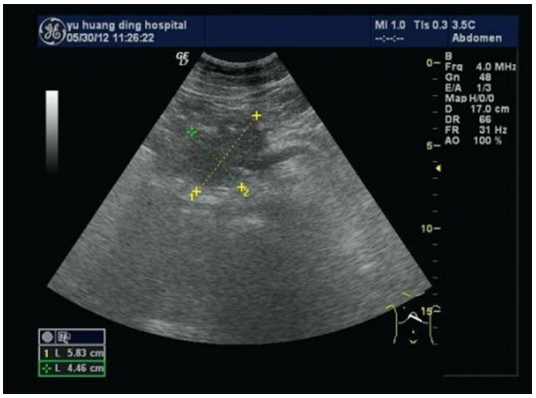

Figure 1. The ultrasound of pancreatic head SPTP patient shows hypoechoic mass of pancreatic head.

measurement data conforming to normal distribution were expressed as ($\bar{x}$ ± s) and compared by paired *t*-test. The counting data were expressed by percentage, and the comparison was analyzed by χ^2 test. Statistical meaning was accepted by $P < 0.05$. Graphpad prism 8 and Photoshop 2018 software were used for drawing.

Results

Clinical data

The observation subjects included 22 females and 8 males aged 34-67 years old, with an average age of (48.37 ± 9.02) years. 18 cases had an abdominal mass accidentally found during physical examination, 12 cases showed epigastric pain, and 3 cases were accompanied by jaundice.

Features of abdominal ultrasound

The size of the pancreatic masses was about 1.5-9.3 cm, which were all single tumors. The tumor type of patients were all single tumors, the masses of 15 patients were located at the body of the pancreas, 12 cases at the tail of the pancreas, and the remaining 3 at the head of the pancreas. Besides, 22 cases had intact capsule, and 8 cases showed infiltrative growth. The masses were founded on the edge of pancreas, with most of which located outside the pancreas. Therefore, although the masses were large, there were only 3 cases of masses located at the head of the pancreas that compress the common bile duct and cause obstructive jaundice. Ultrasonography of 24 patients showed hypoechoic solid cystic masses with insufficient internal blood flow (see **Figure 1**).

The CT finds of SPTP patients presented solid or cystic solid masses. Among which, 15 cases were solid component, 12 cases were cystic component and the remaining 3 cases showed a similar ratio of cystic to solid masses. The outline of the masses was relatively regular, mainly round or elliptical, partly irregular and shallowly lobulated. The density of plain scan was generally lower than that of normal pancreas, and the enhanced scan of the solid parts of the lesion showed uneven mild enhancement in the arterial phase. The enhancement in the portal phase and the delayed phase was higher than that in the arterial phase, showing progressive enhancement; but it was lower than which in the normal pancreas, with no enhancement of cystic part.

Among the 30 masses in experiment, 15 were mainly solid components. The plain scan showed that the density of the tumor was uneven, and mostly which were slightly lower than that of the pancreas, and the cystic parts were mainly distributed around the lesion; 12 cases were mostly cystic components with solid components distributed around the tumor, showing papillary or wall nodular protuberance. After the enhanced scanning, it was found papillary or wall nodular shape, the solid enhanced part was set off by the unnd the plain scanning density was uneven. The enhancement showed enhanced cystic component, showing a “cloudy feature”; there were 3 cases with a similar ratio of cystic and solid components. The cystic and solid parts distributed irregularly at the alternating distribution of reinforced and unreinforced area (**Figure 2**). CT scan showed a cystic solid mass in the body of the pancreas with obvious calcification, which was “eggshell like” (**Figure 2A**). The enhanceed scan showed that the solid part was enhanced while the cystic part was not enhanced (**Figure 2B**).

After enhancement, the arterial phase CT value of the solid part was (45.29 ± 8.39) Hu, and was (50.27 ± 7.28) Hu in parenchymal phase, while the enhanced arterial phase CT value of normal pancreatic tissue was (73.46 ± 12.19) Hu, and was (74.21 ± 13.29) Hu in parenchymal phase. The CT value of enhanced parenchymal phase was significantly higher than that

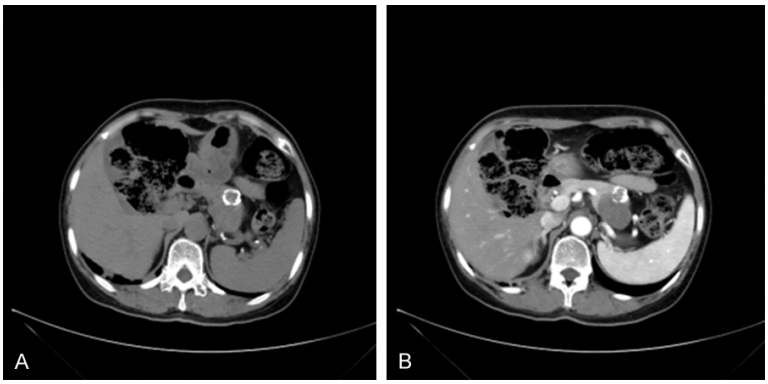

Figure 2. CT scan of SPTP in the body of the pancreas. A. CT scan showed a cystic solid mass in the body of the pancreas with obvious calcification, which was "eggshell like". B. The enhanced scan showed that the solid part was enhanced while the cystic part was not enhanced.

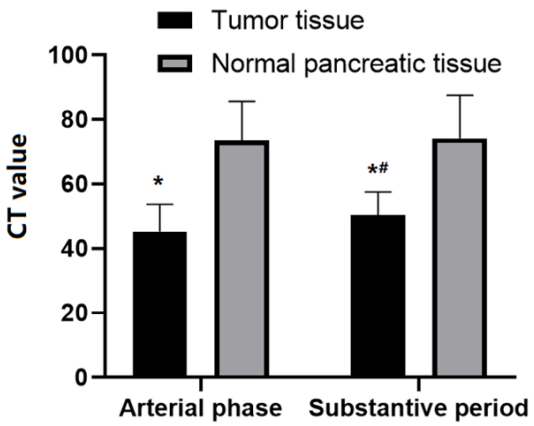

Figure 3. Comparison of enhanced scan CT values between tumor tissue and normal pancreatic tissue. (Note: Comparison with normal pancreatic tissue, $^{*}P < 0.05$; comparison with the arterial phase, $^{\#}P < 0.05$).

of the arterial phase (t=2.456, P=0.017), with the enhancement curve showed a gradual ascending pattern; In addition, the CT values of tumor in both the arterial stage and parenchymal stage were significantly lower than those of normal pancreatic tissue (t=10.426, P=0.000; t=8.653, P=0.000) (**Figure 3**).

Features of MRI

The MRI examination of 30 cases showed that the cystic and solid components were mixed in the lesion. The solid part of T1WI showed an iso-low signal, T2WI showed an iso-high signal, the cystic part T1WI showed a low signal, T2WI showed a high signal. The solid part of the DWI tumor showed limited diffusion and high signal, while the cystic part with non-restricted diffusion showed low signal. The enhanced scanning MR was consistent with that of CT. The tumor and capsule were clearly displayed on MRI. Both plain scan T1WI and T2WI showed iso-low signal, and the enhanced scan showed progressive enhancement of the capsule and cyst wall (**Figure 4**). T1WI showed a low-signal mass on the pancreatic head (**Figure 4A**). The enhanced coronal tumor presented a cystic and solid structure with cystic in the center and solid in the periphery (**Figure 4B**). Enhanced axial scan showed that the tumor was cystic and solid with obvious enhancement (**Figure 4C**).

The patients' EUS showed hypoechoic solid-cystic lesions in the pancreas areas, with inadequate internal blood flow signals. 12 of the 30 patients underwent EUS-guided needle biopsy, which showed different degree of hardness of the lesions during puncture. Among which, 6 cases of lesions were hard in texture and the puncture needle was not easy to penetrate the tumor tissue; 4 cases were soft in texture and blood-like tissue was drawn out; 2 cases were of medium texture and strip-shaped tissue was extracted (**Figure 5**). Annular scan EUS showed the lesion as a cystic mass (**Figure 5A**). EUS puncture biopsy: The blood flow signal in the mass was not rich, and the mass was soft during puncture (**Figure 5B**). A tissue smear examination of similar blood showed a bloody background, with fine fiber vascular bundles and papillary structures, the surrounding coated cells were relatively consistent cells without obvious atypia (**Figure 5C**).

Surgical treatment

Blood vessels were visible on the surface of the tumor during the surgery. Among which, 22 cases were clear and 8 cases adhered to surrounding tissues. In addition, 15 cases underwent complete resection of tumor tissue, 12 cases underwent resection of tumor, partial pancreas and spleen, and 3 cases underwent pancreaticoduodenectomy.

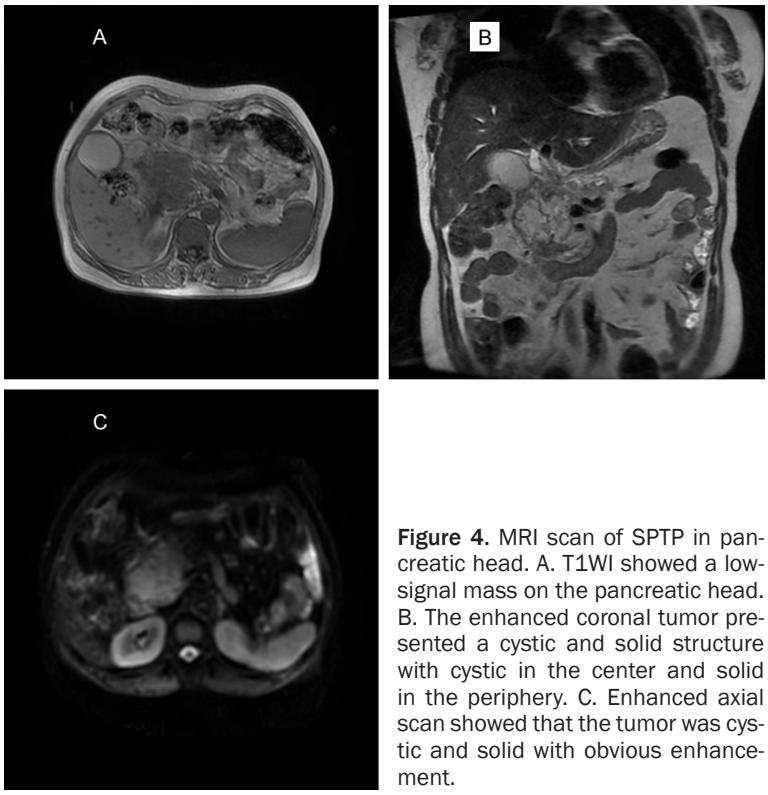

Figure 4. MRI scan of SPTP in pancreatic head. A. T1WI showed a low-signal mass on the pancreatic head. B. The enhanced coronal tumor presented a cystic and solid structure with cystic in the center and solid in the periphery. C. Enhanced axial scan showed that the tumor was cystic and solid with obvious enhancement.

Pathological features

In this group of cases, the tumors had capsules or pseudo-capsules by gross observation. Of which, 22 cases had complete and hard capsules without invasion of pancreatic capsule. 8 cases had unclear boundaries between tumors and surrounding tissues. All specimens showed that the solid and cystic parts were mixed in different ratios, of which 13 were primarily solid components, 12 cases were cystic components, and 5 cases were composed of both cystic and solid components. Microscopically, the tumor cells were in small size and consistent in shape, and the heteromorphosis was not obvious. The tumor cells were round or elliptic, and the typical pseudopapillary structure was often formed around the axis of fibrous vessels. Immunohistochemistry has certain value in the diagnosis of SPTP, but there is no specific diagnostic index at the moment. Vimentin was the most common positive marker in tumor cells. All 30 patients showed positive vimentin with positive CD10 in 22 patients, and the expression of other markers CK, NSE, CK8/18, CgA, and Syn were different (**Figure 6**). The tumor capsule was complete, with cystic solid tissue in it (**Figure 6A**). Conventional HE staining, cystic mass of the pancreas with fibrous cyst wall and extensive necrosis of the contents in the cyst, and part of the necrotic area was papillary (**Figure 6B**). Immunohistochemically positive Vimentin (**Figure 6C**). Immunohistochemically positive CD10 (**Figure 6D**).

Compared the arterial phase CT values of SPTP for patients with different CD10 expression, the arterial phase CT values of patients with positive CD10 expression were significantly lower than those of patients with negative CD10 expression ($P < 0.05$) (**Figure 7**).

Follow-up results

The 30 patients were followed up for 5 to 20 months after surgery. Among them, 3 patients with pancreatic head lesions died of liver metastasis, and the remaining 27 patients were in good condition without recurrence or metastasis.

Discussion

Solid pseudopapillary tumor of pancreas (SPTP) is a rare and low-grade pancreatic tumor, which mostly occurs in adolescent or young women. 22 subjects enrolled in total 30 patients female (73.3%). Since the onset of the disease is closely related to gender and age, the characteristics should be focused on during diagnosis. Many patients were told of pancreatic tumor after physical examination, which caused extreme panic of them. The previous diagnosis of the disease relied on imaging examination (color ultrasound, CT and MRI) [5-8]. With the application of EUS-guided puncture technology in recent years, it can be performed on pancreatic space-occupying lesions to clarify the pathological diagnosis and provide theoretical basis for the selection of surgical treatment [9].

SPTP can occur in any part of the pancreas, and often has a complete or a pseudo capsule [10]. It is likely that the tumor may be

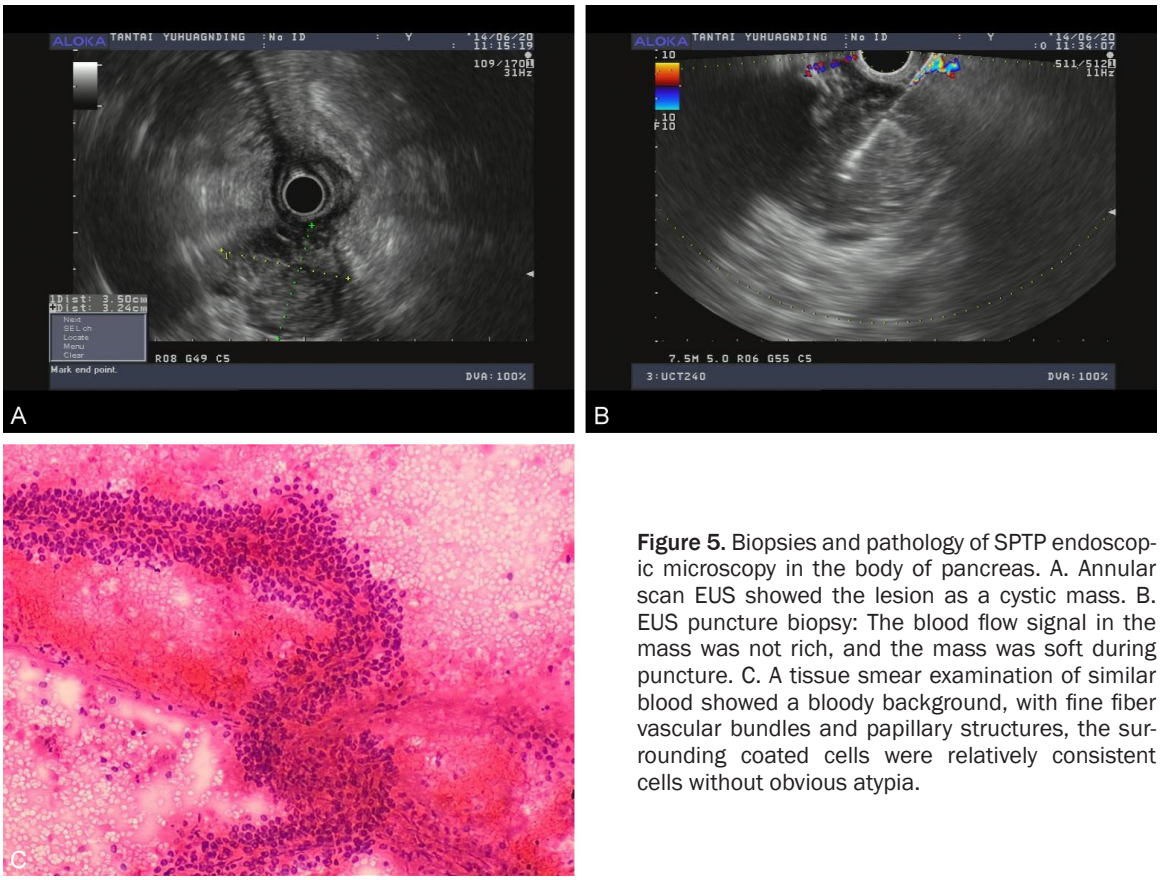

Figure 5. Biopsies and pathology of SPTP endoscopic microscopy in the body of pancreas. A. Annular scan EUS showed the lesion as a cystic mass. B. EUS puncture biopsy: The blood flow signal in the mass was not rich, and the mass was soft during puncture. C. A tissue smear examination of similar blood showed a bloody background, with fine fiber vascular bundles and papillary structures, the surrounding coated cells were relatively consistent cells without obvious atypia.

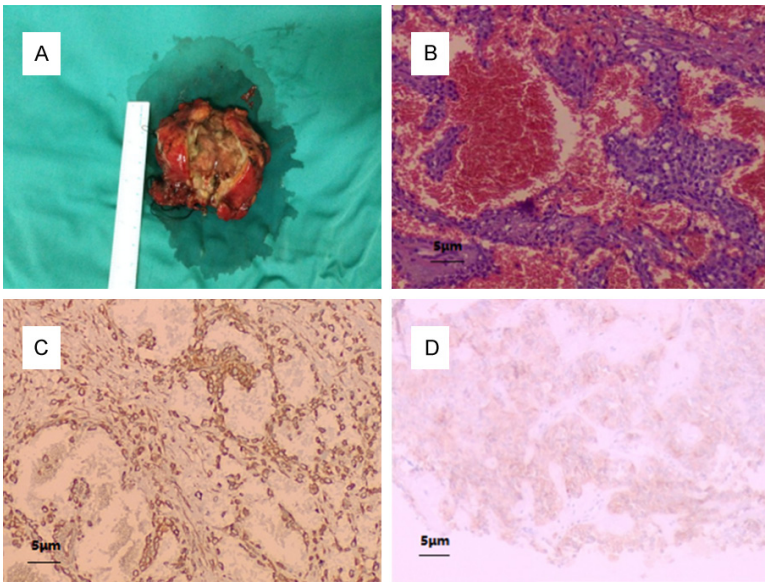

Figure 6. Surgically excised pathological specimens observed by naked eyes and microscope. A. The tumor capsule was complete, with cystic solid tissue in it. B. Conventional HE staining, cystic mass of the pancreas with fibrous cyst wall and extensive necrosis of the contents in the cyst, and part of the necrotic area was papillary. C. Immunohistochemically positive vimentin. D. Immunohistochemically positive CD10.

malignant when it is in irregular shape or invades adjacent tissues. In this study, there were 3 cases of lesions located in the pancreatic head that compressed the common bile duct to cause obstructive jaundice, which resulted in liver metastasis. Besides, among the total 30 cases, the masses were primarily solid in 13 cases, cystic in 12 cases, and similar in cystic and solid components in 5 cases. SPTP has certain similar characteristics in imaging performance as previously reported. Its ultrasound manifestations are cystic-solid masses with low echo and insufficient internal blood flow.

The different tumor components impose different char-

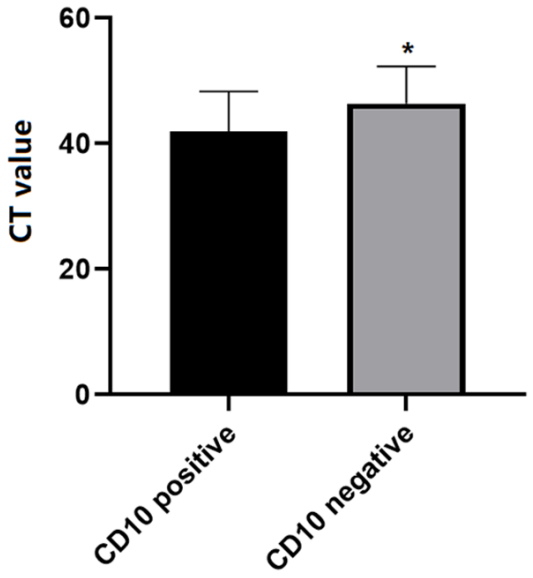

Figure 7. Comparison of tumor CT values of patients with different expressions of CD10. (Note: Comparison with Positive Expression of CD10, $^{*}P < 0.05$).

acteristics on enhanced CT. In this study, there were 13 cases solid tumors with cystic located at the edge of the tumor. The enhancement showed that progressive enhancement in the solid part, while the cystic part was not enhanced; there were 12 cases with cystic components, which distributed around the tumor. The author found that in this group of cases, for solid tumors, the cystic components were distributed around the lesion; while for cystic tumors, the solid parts were distributed around the lesion. Therefore, it was considered that it is due to the squeezing of surrounding tissues when solid components were dominant or when there were more cyclic components. Besides, there were 5 cases with a similar ratio of cystic and solid components. The solid and cystic parts did not have certain distribution characteristics and were mostly distributed irregularly.

In this study, 30 patients underwent MRI examination during the same period. The authors found that MRI was superior to CT in the diagnosis of hemorrhage, cystic components and capsule integrity. Among which, there were 12 cases that showed bleeding signals. The gross specimens suggested focal hemorrhage, but was difficult to be distinguished with CT. Due to the high resolution of soft tissue, MRI was superior to CT in the clarity and integrity of capsule and cystic wall, with the enhanced scan showed progressive enhancement. Meanwhile, by combining with literature reports, the authors speculated that progressive enhancement might be one of the characteristic manifestations of SPTP diagnosis. It was reported in the literature that 1/3 of SPTP cases have calcifications, which mostly occur at the edge of the tumor and are mostly spot-like and line-like calcifications [11]. There were 2 cases of calcification in this study, with the calcification rate of 40%. In accordance with the literature reports, the calcification pattern was mostly spot calcification, among which 1 case showed solid partial calcification of the tumor, showing “eggshell-like” calcification. Studies have shown that the obvious calcification of the solid components is an important feature that distinguishes SPTP from other cystic tumors of the pancreas, and CT is superior to MRI in the diagnosis of calcification [12].

The gross specimen of SPTP is usually round or quasi-circular masses with large volume. It has intact and thick capsule, and the sections have varying degrees of bleeding, necrosis and cystic degeneration. According to pathological findings, SPTP is composed of solid area, pseudopapillary area and the mixed components of the two. Therefore, it is now termed as solid papilloma [13-15]. One of the pathological features of SPTP is that the tumor cells are small, surrounded the axis of the fibrous vessels in nests or lumps shapes to form a characteristic pseudopapillary structure. While the tumor cells that far away from the blood vessels degenerate, undergo necrosis and liquefaction, and then forming the cystic components of masses. The fibrous tissue with necrotic degeneration may have focal calcification, and hemorrhage is easily to occur due to its thin blood vessel wall inside the tumor, which is another characteristic of SPTP [16, 17].

CD10 protein expression has been found in a variety of tumors, which is related to the degree of tumor malignancy and the prognosis of patients [18-20]. In this study, the CT value of patients with different CD10 expressions was compared. CT value of patients with positive CD10 expression was significantly lower than that of patients with negative CD10 expression, suggesting that the expression of CD10 might be related to the solid/cystic component distribution of the tumor. However, it still needs to be further studied and analyzed.

Due to the low incidence rate of the disease and the limited number of patients included, adequate sample research data were failed to be enrolled in this study for analyzing the results. Therefore, in further research, it is necessary to expand the sample size for more in-depth statistical analysis. CT and MRI performance of SPTP has certain characteristics. When a cystic solid tumor with a clear inner boundary of the pancreas is found in young female, the explicit diagnosis can be basically made based on its typical enhancement mode and characteristic changes such as intratumoral hemorrhage, capsule, and calcification. For cases where a definite diagnosis cannot be made, EUS-guided puncture biopsy can be employed to clarify the pathological nature before surgery, which is of great significance for the selection of surgical approaches as well as the evaluation of prognosis.

Disclosure of conflict of interest

None.

Address correspondence to: Liu-Ye Huang, Department of Gastroenterology, The Affiliated Yantai Yuhuangding Hospital of Qingdao University, No. 20 Yudong Road, Zhifu District, Yantai 264000, Shandong, China. Tel: +86-0535-6691999; E-mail: huangliuye8885@163.com

References

[1] Pandey V and Storz P. Targeting the tumor microenvironment in pancreatic ductal adenocarcinoma. Expert Rev Anticancer Ther 2019; 19: 473-482.

[2] Takahashi K, Ehata S, Koinuma D, Morishita Y, Soda M, Mano H and Miyazono K. Pancreatic tumor microenvironment confers highly malignant properties on pancreatic cancer cells. Oncogene 2018; 37: 2757-2772.

[3] Gall TMH, Belete S, Khanderia E, Frampton AE and Jiao LR. Circulating tumor cells and cell-free DNA in pancreatic ductal adenocarcinoma. Am J Pathol 2019; 189: 71-81.

[4] Lee NH, Nikfarjam M and He H. Functions of the CXC ligand family in the pancreatic tumor microenvironment. Pancreatology 2018; 18: 705-716.

[5] Fang JM and Shi J. A clinicopathologic and molecular update of pancreatic neuroendocrine neoplasms with a focus on the new World Health Organization classification. Arch Pathol Lab Med 2019; 143: 1317-1326.

[6] Cui R, Yue W, Lattime EC, Stein MN, Xu Q and Tan XL. Targeting tumor-associated macrophages to combat pancreatic cancer. Oncotarget 2016; 7: 50735-50754.

[7] Vohra R, Park J, Wang YN, Gravelle K, Whang S, Hwang JH and Lee D. Evaluation of pancreatic tumor development in KPC mice using multiparametric MRI. Cancer Imaging 2018; 18: 41.

[8] Zhang YF, Jiang SH, Hu LP, Huang PQ, Wang X, Li J, Zhang XL, Nie HZ and Zhang ZG. Targeting the tumor microenvironment for pancreatic ductal adenocarcinoma therapy. Chin Clin Oncol 2019; 8: 18.

[9] Farran B and Nagaraju GP. The dynamic interactions between the stroma, pancreatic stellate cells and pancreatic tumor development: novel therapeutic targets. Cytokine Growth Factor Rev 2019; 48: 11-23.

[10] Seino T, Kawasaki S, Shimokawa M, Tamagawa H, Toshimitsu K, Fujii M, Ohta Y, Matano M, Nanki K, Kawasaki K, Takahashi S, Sugimoto S, Iwasaki E, Takagi J, Itoi T, Kitago M, Kitagawa Y, Kanai T and Sato T. Human pancreatic tumor organoids reveal loss of stem cell niche factor dependence during disease progression. Cell Stem Cell 2018; 22: 454-467.

[11] Lafaro KJ and Melstrom LG. The paradoxical web of pancreatic cancer tumor microenvironment. Am J Pathol 2019; 189: 44-57.

[12] Lens E, van der Horst A, Versteijne E, Bel A and Tienhoven G. Considerable pancreatic tumor motion during breath-holding. Acta Oncol 2016; 55: 1360-1368.

[13] Pishvaian MJ, Bender RJ, Halverson D, Rahib L, Hendifar AE, Mikhail S, Chung V, Picozzi VJ, Sohal D, Blais EM, Mason K, Lyons EE, Matrisian LM, Brody JR, Madhavan S and Petricoin EF 3rd. Molecular profiling of patients with pancreatic cancer: initial results from the know your tumor initiative. Clin Cancer Res 2018; 24: 5018-5027.

[14] Orozco CA, Martinez-Bosch N, Guerrero PE, Vinaixa J, Dalotto-Moreno T, Iglesias M, Moreno M, Djurec M, Poirier F, Gabius HJ, Fernandez-Zapico ME, Hwang RF, Guerra C, Rabinovich GA and Navarro P. Targeting galectin-1 inhibits pancreatic cancer progression by modulating tumor-stroma crosstalk. Proc Natl Acad Sci U S A 2018; 115: 3769-3778.

[15] Wu J, Li H, Shi M, Zhu Y, Ma Y, Zhong Y, Xiong C, Chen H and Peng C. TET1-mediated DNA hydroxymethylation activates inhibitors of the Wnt/β-catenin signaling pathway to suppress EMT in pancreatic tumor cells. J Exp Clin Cancer Res 2019; 38: 348.

[16] Dougan M, Ingram JR, Jeong HJ, Mosaheb MM, Bruck PT, Ali L, Pishesha N, Blomberg O, Tyler PM, Servos MM, Rashidian M, Nguyen QD, von Andrian UH, Ploegh HL and Dougan SK. Target-

ing cytokine therapy to the pancreatic tumor microenvironment using PD-L1-specific VHHs. Cancer Immunol Res 2018; 6: 389-401.
[17] Xie ZB, Yao L, Jin C and Fu DL. Circulating tumor cells in pancreatic cancer patients: efficacy in diagnosis and value in prognosis. Discov Med 2016; 22: 121-128.
[18] Estrella JS, Li L, Rashid A, Wang H, Katz MH, Fleming JB, Abbruzzese JL and Wang H. Solid pseudopapillary neoplasm of the pancreas: clinicopathologic and survival analyses of 64 cases from a single institution. Am J Surg Pathol 2014; 38: 147-157.
[19] De Robertis R, Paiella S, Cardobi N, Landoni L, Tinazzi Martini P, Ortolani S, De Marchi G, Gobbo S, Giardino A, Butturini G, Tortora G, Bassi C and D'Onofrio M. Tumor thrombosis: a peculiar finding associated with pancreatic neuroendocrine neoplasms. A pictorial essay. Abdom Radiol (NY) 2018; 43: 613-619.
[20] Farr N, Wang YN, D'Andrea S, Gravelle KM, Hwang JH and Lee D. Noninvasive characterization of pancreatic tumor mouse models using magnetic resonance imaging. Cancer Med 2017; 6: 1082-1090.